Neural Networks for Acute Lymphoblastic Leukemia Detection

Airam Curtidor[1], Tetyana Baydyk[2]
[1]Universidad Nacional Rosario Castellanos, Mexico City, Mexico
[2]ICAT, UNAM, Mexico City, Mexico
[1]*curtidor.airam928@rcastellanos.cdmx.gob.mx*, [2]*t.baydyk@icat.unam.mx*

Abstract— **We have developed and present here the method for the detection and classification of white blood cells using microscopic images of peripheral blood smears. It was proposed describing the images using brightness, contrast, and micro-contour orientation histograms. Each of these descriptions provides a coding of the image, which in turn provides *n* parameters. The extracted characteristics are presented to an encoder's input of the neural network. The encoder generates a high-dimensional binary output vector, which is presented to the input of the neural classifier. This paper presents the performance of one classifier, the Random Threshold Classifier (RTC). The classifier's output is the recognized class, which is either a healthy cell or an Acute Lymphoblastic Leukemia-affected cell. The proposed RTC achieved a recognition rate of 98.3 % when the data has partitioned in proportion: 80 % for training set and 20 % for testing set..**

Keywords— RTC neural classifier; image processing; cell analysis; detection of white blood cells; leukemia classification

I. INTRODUCTION

Artificial Intelligence (AI) is currently used in a wide variety of fields, including the medical field. With the aid of various AI techniques, specialized software for the early diagnosis of diseases can be developed [1–3].

In the study [4] AI techniques are applied to analyze and recognize images captured by a microscope of human peripheral blood smear samples. A tool is developed using computer vision and neural networks to help detect possible changes in the size and shape of the different blood cells, with a focus on lymphocytes, for the detection of Acute Lymphoblastic Leukemia (ALL) [4]. The morphological assay can add information about the pathophysiology of COVID-19 disease and its progression. In this type of analysis, hematological abnormalities that occur in patients affected by severe viral pneumonia with clinical consequences that can end in multiple organ failure were detected [5–8].

A normal blood consists of three main components: red blood cells (erythrocytes), white blood cells (WBC) or leukocytes, and platelets. Leukocytes are easily distinguishable due to the fact that their nuclei are darker than the background. Granulocytes are leukocytes containing granules, including neutrophils, basophils, and eosinophils. Cells without granules are called mononuclear and include lymphocytes and monocytes, Fig. **1**. The percentage of lymphocytes in human blood ranges from 20 % to 45 %, and their size ranges from 7 to 15 micrometers. They are distinguished by a round nucleus and poor cytoplasm. ALL affects a group of leukocytes called lymphocytes and is caused by the excessive production of immature white blood cells called lymphoblasts (also known as blastic cells), which inhibit the production of normal white blood cells. ALL lymphoblasts are characterized by additional morphological alterations that exacerbate the severity of the disease. In particular, lymphocytes have a regular shape and a compact nucleus with regular and continuous borders. In contrast, lymphoblasts have an irregular shape and contain small cavities in the cytoplasm, called vacuoles, and spherical particles within the nucleus, called nucleoli [9]. Leucocyte classification for leukemia detection using Image Processing Techniques (IPT) was proposed in [10].

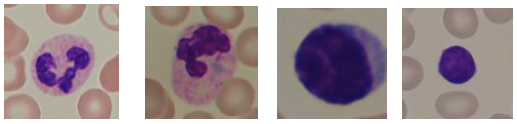

a *b* *c* *d*

Fig. 1. Examples of white blood cells (leukocytes):
a – neutrophils, *b* – basophils,
c and *d* – lymphocytes with ALL [4]

Cells in human blood can be counted using image processing techniques, which at the same time may provide information on cell morphology. A system for the automatic detection of ALL-affected cells is first based on image acquisition using a camera attached to a microscope. The most challenging task in image processing is the segmentation of complex images, such as blood cells, due to their complex nature and overlapping of these cells. Then from each cellular component, different characteristics, such as shape, color, and/or texture as well as their combinations, most of which are problem-specific, are extracted, and the classifier will detect ALL-affected lymphocytes or not from this data.

The problem of white blood cell identification and classification is focused in [11]. The proposed system first separates leukocytes from other blood cells in the blood image, then extracts morphological indices, and finally classifies the leukocytes using a neural classifier. To improve the image, low-pass, and band-pass filters are applied to reduce noise if they do not have good illumination [12]. The authors focus on the segmentation process of blood images to extract significant parts or regions of interest and propose an

DOI: 10.25045/SPCDH4.0.2025.34

intuitionistic fuzzy set approach for optimal threshold selection based on histogram calculations.

Using active contour models that are initialized with morphological operators, cells are segmented in [13]. Functions based on shape and texture are used for classification. An effective technique for automatically segmenting blood cell nuclei is described in [14]. The technique is based on the enhancement and filtering of grayscale contrast. A very detailed review of the different proposals reported in the literature on methods of segmentation, extraction of characteristics, and classification of white blood cells or leukocytes is presented in [15] – [17].

Various segmentation techniques, such as, Hough transform, thresholding techniques, boundary-based segmentation, and region-based segmentation, have been proposed to achieve efficient and accurate results [18–20].

Tests on public datasets for leukemia detection, SMC-IDB, IUMS-IDB, and ALL-IDB, were conducted and achieved an ALL-classification accuracy of 94.1 % [21],

One of the ways to increase the accuracy and speed of recognition algorithms is to use a convolutional neural network (CNN). It was introduced a CNN in conjunction with a Kohonen network, the first to provide the system with the ability to detect and recognize objects and the second to find areas of interest. The combination of the above methods allows to speed up the process of searching and recognizing objects in images [22, 23].

I is important to emphasize that all of the listed works use different methods for the recognition and classification of images of healthy and ALL-affected blood cells. In this work let's present our neural classifier called Random Threshold Classifier (RTC), as well as our approach of the extraction of texture features. The task of medical images recognition is actual and important.

II. MATERIALS AND METHODS

There are different proposals to detect ALL using different artificial intelligence methodologies. They use the ALL-IDB database [24]. This database is popular to compare different methods and algorithms. Let's analyze the results that were obtained with this image database.

There were algorithms and showed the classification of the acute lymphoblastic leukemia into its three respective categories namely: L1, L2, L3, achieved an overall accuracy of 98.6 % [25].

It was used fuzzy c-means (FCM) clustering for nuclei segmentation [26]. They extracted, five geometrical features (area, perimeter, solidity, eccentricity and extent) and, 36 statistical features (mean, standard deviation, energy, entropy, skewness and kurtosis) are calculated from the image histogram of the red, green and blue, plus the hue, saturation and enhanced value channels from the pixels located in nuclei, respectively. In this way they obtained 41 components and selected 13 of the best features. For the classification of L1, L2, L3, normal, reactive and atypical cells, Random Forest (RF) classifier was applied and result was in 98 % accuracy.

It was proposed a hybrid model based on deep convolutional neural networks (CNNs) and a deep residual network named ResNet-50 V2 [27], to predict ALL. They trained the deep residual network using the optimized hyperparameters by genetic algorithms (GA), reaching higher performance against approaches without optimization and optimization using random search and Bayesian algorithms [28]. The results show that the GA optimization improves the accuracy of the classifier, obtaining 98.46 %.

The authors did two experiments: in one of them they obtained 98.62 % when the data has been partitioned on training and testing sets as 80 % and 20 %, and in the second experiment they obtained 97.73 % when the data has been partitioned as training and testing images as 60 % and 40 % [29].

It was proposed an improved Adaptive Network-Based Fuzzy Inference Systems (ANFIS) model to predict leukemia data using an Euclidean distance to measure between the trained feature data and the test feature data [30]. Improved ANFIS obtained the best accuracy of 97.14 %.

Classification of white blood cells into healthy and unhealthy using Support Vector Machine (SVM) learning model was presented in [31]. Image features are extracted with transfer learning approach of deep convolutional neural network using AlexNet pretrained model. AlexNet is an eight layered convolutional neural network. This model is introduced by Alex Krizhevsky at University of Torento in 2010 [32]. This approach validates the process of discriminating white blood cells into healthy and acute lymphoblastic leukemia affected unhealthy cells with 96.15 % of accuracy.

A computer-aided automated diagnosis system for detection of acute lymphoblastic leukemia (ALL) using deep-learning models is discussed in [33]. The work implemented in this paper does not require any preprocessing, the raw image is fed in this model for performing both feature extraction and classification task. This proposed method achieves an accuracy of 98 %.

A micro-pattern descriptor, called Local Directional Number Pattern (LDNP) along with Multi-scale Weber Local Descriptor (MWDT) for feature extraction task to determine cancerous and noncancerous blood cells are discussed and presented in [34].

The k-means clustering algorithm for segment the images. Based on the colour, texture and shape the image pixels are grouped as three clusters. The texture features were extracted as Grey Level Co-Occurrence Matrix (GLCM) and Local Binary Pattern (LBP) are used in [35]. Support vector machine (SVM) with Gaussian radial basis function (RBF) as kernel is used for classification. They obtained an accuracy of 95.3 % for ALL-IDB2 database.

So, last year's active attention of scientists and engineers is attracted to the problem of automatic recognition and classification of blood cells for different types of diseases. Analysis of WBC from blood can help to detect ALL, COVID-19 disease or other illness.

We have proposed an automated method for the identification and classification of white blood cells using microscopic images of peripheral blood smears and neural Random Threshold Classifier (RTC) [36] and Limited Receptive Area (LIRA) Neural Classifier [37] that we do not describe here in detail.

The aim of this study is to develop a method for automated classification of blood cell images for the diagnosis of various diseases, which allows increasing the recognition rate in the diagnosis of diseases. To achieve the goal, the following tasks are required:

– the development of algorithms of feature extraction from images;

– the development of neural networks as element of decision making;

– programming of the algorithms of feature extraction from images and neural network method;

– testing them on selected image database.

Assumptions accepted in the work are the following:

– it is possible to extract different features of the images of the blood as from patients with diseases and from images of healthy persons;

– neural network can be trained and after that can be used to recognize new images of blood cells.

III. Results and Discussion

A. Texture Recognition in Blood Smear Images

The task of image recognition of lymphocytes affected by ALL consisted from several steps. The first step requires selecting the cells that are affected by the disease. A typical blood image consists of three components: red blood cells (erythrocytes), leukocytes, and platelets. Therefore, let's focus on leukocytes, specifically lymphocytes. Fig. 2 depicts a sample image from the ALL-IDB2 database [24] containing two healthy cells from patients without ALL and two probable blast cells. The second step includes the calculation of texture features. The third step includes the training of neural classifier.

The method of French-American-British co-operative group (FAB) is used in medicine for a long time to classify a cell as a blast or normal [38]. The FAB classification for acute lymphoblastic leukemia is divided into three categories:

L1: Lymphoblasts are small and homogeneous. The nuclei are round and regular with little cleavage and discrete nucleoli. The cytoplasm is scant and usually without vacuole.

L2: Lymphoblasts are massive and diverse. The nuclei are irregular and frequently cleft. Nucleoli are present. The cytoplasm may contain vacuoles, and its volume is variable but typically abundant.

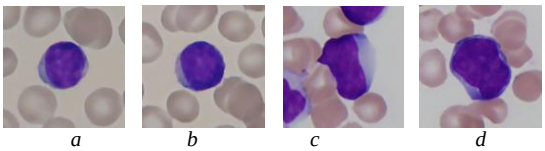

a *b* *c* *d*

Fig. 2. Images from the ALL-IDB2 database [24]:
a and *b* present healthy cells from patients without ALL;
c and *d* present probable lymphoblasts from patients with ALL

L3: Lymphoblasts range in size from moderate to large and are homogeneous. One or more prominent nucleoli are present. The shape of the nuclei is regular and round-oval. The cytoplasm is moderate in volume and contains numerous prominent vacuoles.

The RTC includes the following blocks: Input data, Characteristic extractor, Encoder, Classifier, and Recognition class (ALL cells or Normal cells). The extracted characteristics are presented to the input of the encoder. The encoder generates the output binary vector, which is then presented to the input of the single-layer neural classifier, and, finally, the classifier's output provides the recognized class, which in this case consists of two classes, healthy cell, and affected cell [36, 39, 40].

B. Caracteristic Extractor

This module is based on the image processing procedure. It provides with the necessary information to distinguish a leukocyte from the other cells in the peripheral blood image, as well as the characteristics that distinguish a lymphocyte from a lymphoblast. This system includes color, texture, and border characteristics represented through their histograms, and these characteristics are obtained from the nucleus of every lymphocyte or lymphoblast discovered by the system. To achieve this, an initial image is scanned by moving a (20×20)-pixel window with a 10-pixel step. Three brightness, contrast, and contour orientation histograms were calculated for each window. Each histogram consists of 16 components, for a total of 48 components or features that will comprise the input vector $\boldsymbol{X}$ for the RTC classifier.

C. Caracteristic Encoder

The characteristic encoder converts the extracted properties given by the property or characteristics extractor into a binary vector. Encoding then creates a binary vector *b* for all blocks. This vector is presented as the classifier's first layer. The proposed classifier's first layer follows the same training rule as a one-layer perceptron.

D. Random Threshold Classifier (RTC)

It is proposed a neural classifier with high performance both in training and processing. Random Threshold Classifier (RTC) is the name of this classifier [39, 40]. The basic idea is to create multilayer perceptrons with a single layer of training connections, which allows a rapid training rate. Placing additional non-modifiable layers of connections and binary neurons that allow nonlinear transformations of spatial input parameters to binary spatial parameters with extremely high

dimensions improves image recognition accuracy.

The RTC structure is depicted in Fig. 3. The network structure is comprised by *s* similar blocks with a neural output in each block. A complete set of *X* input characteristics supplies each block's inputs.

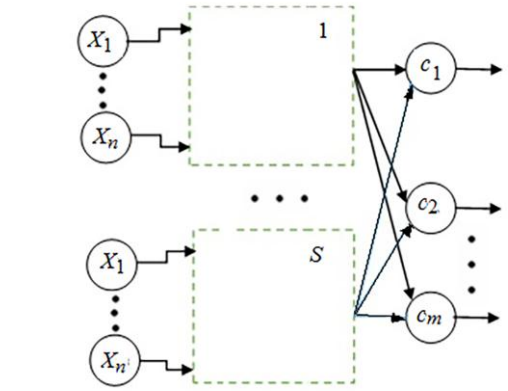

a

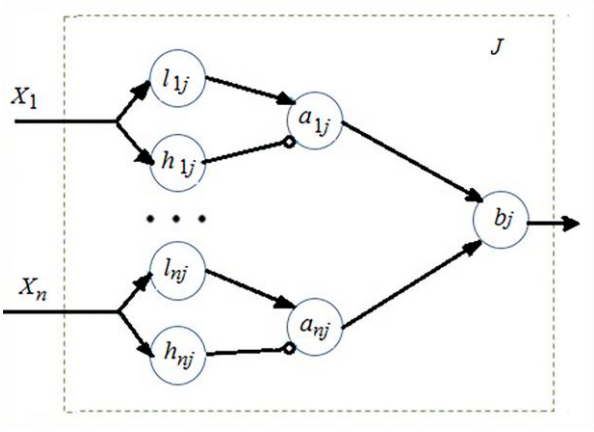

b

Fig. 3. Random threshold neural classifier: *a* – the whole structure; *b* – structure of one block

Now let's describe the one block functioning (Fig. 3, *b*). Each *X* characteristic feeds two neurons, one neuron with high threshold (*h*) and other neuron with low threshold (*l*), where *S* represents the number of neuron blocks. The low threshold value falls always below the high threshold value. A unique random procedure determines these values. The output of the neuron with low threshold is connected to the excited input of the next neuron *a*, and the output of the neuron with high threshold is connected to the inhibited output of the next neuron *a*. At the output of *a* neuron, the signal only occurs when the input signal *X* is between low and high values of thresholds. All outputs of *a* neurons within a *j* block are connected to the excited inputs of *b* output neuron, which represents the whole neural block output.

The *b* neuron is analogue of a logical element "And" i. e., in the *b* neural output, the signal is generated when all *a* neurons within the block are excited. The neural output for each block is connected to all the neural inputs of the last layer *c* of the classifier through trainable connections. The *c* neuron in the last or response layer are associated with class to be recognized. The weights of trainable connections between *b* and *c* neurons are modified at each training stage. Each *c* neuron represents a classification response of the system, and the neuron with the greatest excitation value is chosen as classifier response.

The classifier works in two ways: training and recognition. For training connections, Hebbian's rule is applied.

$$w_{jc}(t+1) = w_{jc}(t) + a, \tag{1}$$

$$w_{ji}(t+1) = w_{ji}(t) - a, \tag{2}$$

in which the *c* index represents the correct class, and the index *i* represents the incorrect class.

The neural network undergoes a training phase whose objective is to correctly recognize as many patterns as possible. The training consists of decreasing all the weights of the connections of the incorrect class and increasing those of the correct class, which leads us to supervised or master training.

In order to understand the principles mentioned above, let's interpret them geometrically, as shown in Fig. 4, for a case with three input variables X_1, X_2, and X_3, so for three-dimension task instead of *n* dimension as presented in Fig. 3.

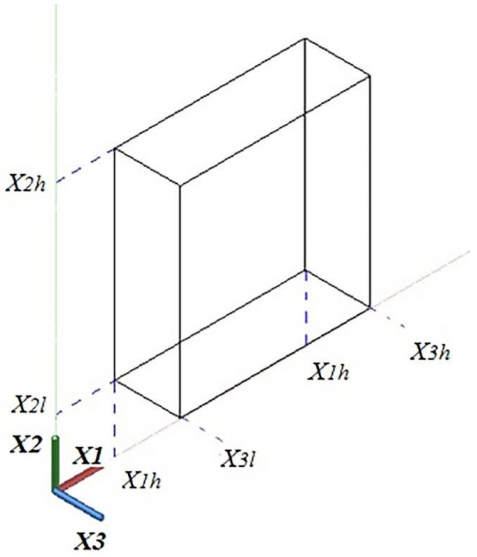

Fig. 4. Geometric identification of the neuron

When the point representing the feature vector is inside the represented rectangle, the output neuron that is corresponded to the block output will be stimulated or active. Since the classifier contains a sufficient number of blocks with similar (neurons with thresholds) but different characteristics (different values of thresholds), all spatial features appear in a sufficient number of multidimensional parallelepipeds located on random planes and having random sizes. Let's demonstrate the geometrical interpretation only for three input parameters.

The number of parallelepipeds is equal to the number of blocks. It is possible to analyze the point in space $\left(X_1^*, X_2^*, X_3^*\right)$ shown in Fig. 5 where numerous (*V*) parallelepipeds have been covered. With the training process and definition of weights between penultimate and last layers the neural classifier can divide the parametric space on different classes.

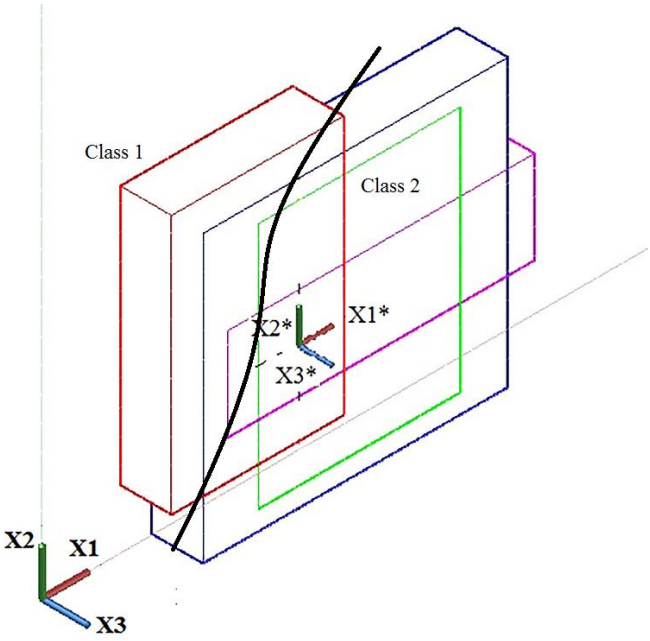

Fig. 5. A geometric representation of the classifier

Taking into account the need to distinguish three classes, let the point $\left(X_1^*, X_2^*, X_3^*\right)$ belong to the second class. If the point is far from the class boundary, it is covered by parallelepipeds whose volumes lie within the class boundary of the second class. This implies that during the training process, the weights of the connections between neurons *b* and *c* will contribute to the second class. Therefore, the point $\left(X_1^*, X_2^*, X_3^*\right)$ will be recognized as belonging to the second class.

E. Database Descriprion:ALL-IDB

ALL-IDB [24] is a public imaging database of peripheral blood samples from healthy individuals and leukemia patients. These samples were gathered by professionals at the M. Tettamanti Research Center for Childhood Leukemia and Hematological Diseases in Monza, Italy. The ALL-IDB database is comprised of two different versions, ALL-IDB1 and ALL-IDB2, and its images are in JPG format with 24-bit color depth. ALL-IDB1 is comprised of 108 original RGB images captured with a laboratory optical microscope and an Olympus Optical C2500L camera or a Canon Power Shot G5 camera. The resolution of the first 33 images is 1712×1368, while the remaining images have a resolution of 2592×1944.

The images were taken at different microscope magnifications, ranging from 300 to 500, which brought the differences in color and brightness. ALL-IDB1 provides complete images containing cells and agglomerates; thus, it can be used to evaluate the segmentation capabilities of algorithms, as well as the image preprocessing techniques or the classification systems. ALL-IDB2 is a collection of clipped areas of interest from blastic and healthy cells extracted from ALL-IDB1. It consists of 260 images, with 50 % of these depicting lymphoblasts.

F. Comparison of Results

To present the results obtained by the RTC neural classifier, the aforementioned ALL-IDB2 database was employed, along with 100 images, of which 60 were used for training and the remaining 40 for testing.

The graphical user interface is comprised of a menu with the following options: Fig. 6: Mask generation, Open Image-Coding, Training, and Recognition.

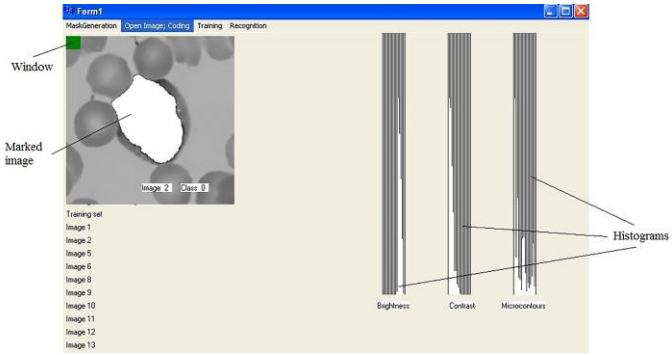

Fig. 6. Principle menu and scan of image with 20x20 window

In the first option, "Mask generation" is the first part of the RTC classifier structure. The program randomly selects images from the ALL-IDB database for the training phase, where half of the images are selected for training and the other half for testing. The following option – "Open Image-Coding"– is where the 100 images in the database are opened and encoded. It is performed a scan of a (20×20) pixels window. Where there are three classes, one of them corresponds to class zero (0), which helps us identify the background of the image; the next class (1) for the case where there are no cells affected by the ALL disease, i.e., healthy cells, and finally, class two (2) where there are cells affected by the ALL disease (lymphoblasts). For each of these classes, the histograms of brightness, contrast, and micro-contour orientation for the window are computed, and thereafter those data are codified.

Once this process is finished, the "Training" option will begin, which, as mentioned above, consists of decreasing all the weights of the connections of the incorrect class and increasing those of the correct class, the objective of which is to correctly recognize the most significant number of patterns. Finally, there is the "Recognition" option in which the remaining half of the images, which were not used in the

training phase, are used. At this stage, it is possible to visualize the number of errors, and with these, it is possible to calculate the recognition percentage of our system. It is worth mentioning that to obtain 48 texture characteristics of the area of interest which is the nucleus, as shown in Fig. 6.

Experiments with RTC demonstrate that the results were superior to the best result obtained in [34] and significantly superior to those obtained using SVM-G in [35]. It should be noted that all mentioned methods utilize the ALL-IDB database.

The RTC neural classifier demonstrated a higher recognition percentage of 98.3 % compared with 95.3 % of the SVM-G and of 97.69 % [36, 41]. So our neural classifier may be used to identify the lymphoblasts using images of the healthy or diseased cells. The LIRA demonstrated the best recognition rate of 96.56% [37].

As shortcomings of this study it is possible to note that it is used only one image database. For effective application of neural classifiers it is very important to increase the number of images for training process. The time of training may demand hours or days. But it is possible to use pre-trained neural networks.

IV. CONCLUSIONS

The neural classifier with the title the Random Threshold Classifier (RTC) was used to recognize the texture of human blood cells images, with a focus on white blood cells (leukocytes). The classification of healthy lymphocytes and diseased lymphocytes, also known as lymphoblasts was selected as test task. At the input of the RTC classifier, brightness histograms, contrast histograms, and micro-contour orientation histograms were calculated for each image from the ALL-IDB database, generating a characteristics vector that would be the input of the neural classifier. The specialized program is developed using C++ to extract the characteristics of interest and to train and test the images with RTC neural classifier. The program system permits us to recognize where the healthy or diseased cells are detected. The RTC neural classifier demonstrated a higher recognition percentage of 98.3 % . So our neural classifier may be used to identify the lymphoblasts using images of the healthy or diseased cells. The LIRA demonstrated the best recognition rate of 96.56%.

ACKNOWLEDGMENT

The authors would like to thank Labati et al for sharing the Acute Lymphoblastic Leukemia image database (ALL-IDB).

The special acknowledgment from Dra. Airam Curtidor for poststudent grant SECIHTI, Mexico.

REFERENCES

[1] C. González, "Recognition of Textures in Medical Images". UNAM. 2011. Available at: https://xdoc.mx/documents/tesis-unam-5ddae474b690d

[2] M. Mammadova, N. Bayramov, Z.Jabrayilova, "Development of the principles of fuzzy rule-based system for hepatocelular carcinoma staging", EUREKA: Physics and Engineering, 3, 2021, pp. 3–13. doi: https://doi.org/10.21303/2461-4262.2021.001829

[3] M. Mammadova,, Z. Jabrayilova, "Synthesis of decision making in a distributed intelligent personnel health management system on offshore oil platform", EUREKA: Physics and Engineering, 4, 2022, pp. 179–192. doi: https://doi.org/10.21303/2461-4262.2022.002520

[4] J. Huerta Aragonés, E. E. Cela de Julián, "Practical Hematology: Interpretation of the Complete Blood Count and Coagulation Tests", 2019, Madrid: Lúa Ed. 3.0, 507–528.

[5] M. S. Rahi V., Jindal, S.-P. Reyes, K. Gunasekaran, R. Gupta, I. Jaiyesimi, "Hematologic disorders associated with COVID-19: a review. Annals of Hematology", 100 (2), 2021, pp. 309–320. doi: https://doi.org/10.1007/s00277-020-04366-y

[6] G. Zini, S. Bellesi, F. Ramundo, G. d'Onofrio, "Morphological anomalies of circulating blood cells in COVID-19", American Journal of Hematology, 95 (7), 2020, pp. 870–872. doi: https://doi.org/10.1002/ajh.25824

[7] C. Salib, P. Khattar, J. Cheng, J. Teruya-Feldstein, "Atypical Peripheral Blood Cell Morphology in COVID-19 (Sars-CoV-2) Patients from Mount Sinai Health System in New York City". Blood, 136, 2020, pp. 26–27. doi: https://doi.org/10.1182/blood-2020-142581

[8] G. Introcaso, M. L. Biondi, "Morphological anomalies of blood cells in COVID-19 patients", Open J Clin Med Images, 2 (2), 2022, 1080. Available at: https://www.jclinmedimages.org/articles/OJCMI-v2-1080.pdf

[9] Guía de Referencia Rápida Diagnosis and Treatment Lymphoblastic Leukemia Acute In The Adult. Instituto Mexicano del Seguro Social. Dirección de Prestaciones Médicas. Unidad de Atención Médica. Coordinación de Unidades Médicas de Alta Especialidad. División de Excelencia Clínica, 2018 .

[10] L. Putzu, G. Caocci, C. Di Ruberto, "Leucocyte classification for leukaemia detection using image processing techniques", Artificial Intelligence in Medicine, 62 (3), 2014, pp. 179–191. doi: https://doi.org/10.1016/j.artmed.2014.09.002

[11] V. Piuri, F. Scotti, "Morphological classification of blood leucocytes by microscope images", 2004 IEEE International Conference On Computational Intelligence for Measurement Systems and Applications, 2004. doi: https://doi.org/10.1109/cimsa.2004.1397242

[12] C. D. Ruberto, L. Putzu, "Accurate Blood Cells Segmentation through Intuitionistic Fuzzy Set Threshold", 2014 Tenth International Conference on Signal-Image Technology and Internet-Based Systems, 2014. doi: https://doi.org/10.1109/sitis.2014.43

[13] G. Ongun, U. Halici, K. Leblebicioglu, V. Atalay, M. Beksac, S. Beksac, "An automated differential blood count system", 2001 Conference Proceedings of the 23rd Annual International Conference of the IEEE Engineering in Medicine and Biology Society. 2001. doi: https://doi.org/10.1109/iembs.2001.1017309

[14] M. Mohamed, B. Far, A. Guaily, "An efficient technique for white blood cells nuclei automatic segmentation", 2012 IEEE International Conference on Systems, Man, and Cybernetics (SMC), 2012. doi: https://doi.org/10.1109/icsmc.2012.6377703

[15] E. A. Mohammed, M. M. A. Mohamed, B. H. Far, C. Naugler, "Peripheral blood smear image analysis: A comprehensive review", Journal of Pathology Informatics, 5 (1), 2014, 9. doi: https://doi.org/10.4103/2153-3539.129442

[16] H. T. Madhloom, S. A. Kareem, H. Ariffin, A. A. Zaidan, H. O. Alanazi, B. B. Zaidan, "An Automated White Blood Cell Nucleus Localization and Segmentation using Image Arithmetic and Automatic Threshold", Journal of Applied Sciences, 10 (11), 2010, pp. 959–966. doi: https://doi.org/10.3923/jas.2010.959.966

[17] N. H. A. Halim, M. Y. Mashor, R. Hassan, "Automatic Blasts Counting for Acute Leukemia Based on Blood Samples", Intern. J. of Research and Reviews in Computer Science, 2 (4), 2011, pp. 971–976. Available at: https://www.proquest.com/scholarly-journals/automatic-blasts-counting-acute-leukemia-based-on/docview/903775031/se-2

[18] J. A. Tang, "A color image segmentation algorithm based on region growing", 2010 2nd International Conference on Computer Engineering and Technology, 2010. doi: https://doi.org/10.1109/iccet.2010.5486012

[19] E. Navon, O. Miller, A. Averbuch, "Color image segmentation based on adaptive local thresholds", Image and Vision Computing, 23 (1),

2005, pp. 69–85. doi: https://doi.org/10.1016/j.imavis.2004.05.011

[20] A. I. Mahameed, M. K. Ahmed, N. B. Abdullah, “Iris recognition method based on segmentation”, EUREKA: Physics and Engineering, 2, 2022, pp. 166–176. doi: https://doi.org/10.21303/2461-4262.2022.002341

[21] C. Di Ruberto, A. Loddo, G. Puglisi, “Blob Detection and Deep Learning for Leukemic Blood Image Analysis”, Applied Sciences, 10 (3), 2020, 1176. doi: https://doi.org/10.3390/app10031176

[22] V. Skuratov, K. Kuzmin, I. Nelin, M. Sedankin, “Application of a convolutional neural network and a kohonen network for accelerated detection and recognition of objects in images”, EUREKA: Physics and Engineering, 4, 2020, pp. 11–18. doi: https://doi.org/10.21303/2461-4262.2020.001360

[23] V. Skuratov, K. Kuzmin, I. Nelin, M. Sedankin, “Application of kohonen self-organizing map to search for region of interest in the detection of objects”, EUREKA: Physics and Engineering, 1, 2020, pp. 62–69. doi: https://doi.org/10.21303/2461-4262.2020.001133

[24] R. D. Labati, V. Piuri, F. Scotti, “All-IDB: The acute lymphoblastic leukemia image database for image processing”, 2011 18th IEEE International Conference on Image Processing, 2011. doi: https://doi.org/10.1109/icip.2011.6115881

[25] V. Acharya, P. Kumar, “Detection of acute lymphoblastic leukemia using image segmentation and data mining algorithms”, Medical & Biological Engineering & Computing, 57 (8), 2019, pp. 1783–1811. doi: https://doi.org/10.1007/s11517-019-01984-1

[26] P. Mirmohammadi, M. Ameri, A. Shalbaf, “Recognition of acute lymphoblastic leukemia and lymphocytes cell subtypes in microscopic images using random forest classifier”, Physical and Engineering Sciences in Medicine, 44 (2), 2021, pp. 433–441. doi: https://doi.org/10.1007/s13246-021-00993-5

[27] K. He, X. Zhang, S. Ren, Sun J., “Identity Mappings in Deep Residual Networks”, Lecture Notes in Computer Science, 2016, pp. 630–645. doi: https://doi.org/10.1007/978-3-319-46493-0_38

[28] L. F. Rodrigues, A. R. Backes, B. A. N. Travençolo, G. M. B. de Oliveira, “Optimizing a Deep Residual Neural Network with Genetic Algorithm for Acute Lymphoblastic Leukemia Classification”, Journal of Digital Imaging, 35 (3), 2022, pp. 623–637. doi: https://doi.org/10.1007/s10278-022-00600-3

[29] S. Chand, V. P. Vishwakarma, “A novel Deep Learning Framework (DLF) for classification of Acute Lymphoblastic Leukemia”, Multimedia Tools and Applications, 81 (26), 2022, pp. 37243–37262. doi: https://doi.org/10.1007/s11042-022-13543-2

[30] M. A. Rejula, S. Amutha, G. M. Shilpa, “Classification of acute lymphoblastic leukemia using improved ANFIS”, Multimedia Tools and Applications, 82 (23), 2023, pp. 35475–35491. doi: https://doi.org/10.1007/s11042-023-15113-6

[31] T. V. Renuka, B. Surekha, “Acute-Lymphoblastic Leukemia Detection Through Deep Transfer Learning Approach of Neural Network”, Lecture Notes in Networks and Systems, 2021, pp. 163–170. doi: https://doi.org/10.1007/978-981-33-4073-2_17

[32] G. Litjens, T. Kooi, B. E. Bejnordi, A. A. Setio, F. Ciompi, M. Ghafoorian, J. A. W. M. van der Laak, “A survey on deep learning in medical image analysis”, Medical Image Analysis, 42, 2017, pp. 60–88. doi: https://doi.org/10.1016/j.media.2017.07.005

[33] A. Alam, S. Anwar, “Detecting Acute Lymphoblastic Leukemia Through Microscopic Blood Images Using CNN”, Trends in Wireless Communication and Information Security, 2021, pp. 207–214. doi: https://doi.org/10.1007/978-981-33-6393-9_22

[34] S. H. Wady, “Classification of Acute Lymphoblastic Leukemia through the Fusion of Local Descriptors”, UHD Journal of Science and Technology, 6 (1), 2022, pp. 21–33. doi: https://doi.org/10.21928/uhdjst.v6n1y2022.pp21-33

[35] S. Alagu, K. B. Bagan, “Acute Lymphoblastic Leukemia diagnosis in microscopic blood smear images using Texture features and SVM classifier#, Alliance International Conference on Artificial Intelligence and Machine Learning (AICAAM), 2019,.pp. 175–186. Available at: https://www.researchgate.net/publication/343444613_Acute_Lymphoblastic_leukemia_diagnosis_in_microscopic_blood_smear_images_using_texture_features_and_SVM_classifier

[36] A. Curtidor, E. Kussul, T. Baydyk, M. Mammadova, “Analysis and automated classification of images of blood cells to diagnose acute lymphoblastic leukemia”, EUREKA: Physics and Engineering, N5, 2023, pp. 177-190. doi: http://doi.org/10.21303/2461-4262.2023.003070

[37] A. Curtidor, T. Baydyk, E. Kussul, “Classification Based on Neural Networks to Detect Acute Lymphoblastic Leukemia”, WSEAS Transactions on Signal Processing, Vol. 21, 2025, pp. 25-30. DOI.10.37394/232014.2025.21.4

[38] Bennett, J. M., Catovsky, D., Daniel, M.-T., Flandrin, G., Galton, D. A. G., Gralnick, H. R., Sultan, C. (1976). Proposals for the Classification of the Acute Leukaemias French-American-British (FAB) Co-operative Group. British Journal of Haematology, 33 (4), 451–458. doi: https://doi.org/10.1111/j.1365-2141.1976.tb03563.x

[39] Baidyk, T., Kussul, E., Makeyev, O. (2005). Texture Recognition with Random Subspace Neural Classifier. WSEAS Transactions on Circuits and Systems, 4 (4), 319–324.

[40] Baidyk, T., Kussul, E., Makeyev, O. (2008). General purpose image recognition systems based on neural classifiers. Progress in Neurocomputing Research. Chap. 3. NOVA Publishers, 83–114.

[41] Gayathri, S., Jyothi, R. L. (2018). An Automated Leucocyte Classification for Leukemia Detection. International Research Journal of Engineering and Technology (IRJET), 5 (5), 4254–4264. Available at: https://www.irjet.net/archives/V5/i5/IRJET-V5I5908.pdf